Polymer Chemistry

Accepted Manuscript

ROYAL SOCIETY OF CHEMISTRY

www.rsc.org/polymers

Cite this: DOI: 10.1039/c0xx00000x

www.rsc.org/xxxxxx

ARTICLE TYPE

Core cross-linked polyphosphoester micelles with folate-targeted and acid-cleavable features for pH-triggered drug delivery

Jian Hu, Jinlin He, Dongling Cao, Mingzu Zhang, Peihong Ni*

Received (in XXX, XXX) Xth XXXXXXXXX 20XX, Accepted Xth XXXXXXXXX 20XX

DOI: 10.1039/b000000x

To prevent the disassembly of drug-loaded micelles under the high dilution conditions of the bloodstream, one of the efficient methods is to achieve the cross-linkage inside the micellar core. In this study, we have developed a kind of novel folate-conjugated core cross-linked polyphosphoester micelles with acid-cleavable acetal groups (ACCL-FA). These polyphosphoester-based cross-linked micelles possessed much smaller size and enhanced stability compared to the uncross-linked (UCL) counterpart, and also showed good biodegradability and low cytotoxicity. The *in vitro* release studies revealed that the doxorubicin (DOX)-loaded ACCL micelles showed excellent stability with minimal drug release under neutral conditions, and displayed fast micellar dissociation and drug release in the presence of acid or phosphodiesterase I (PDE I). Moreover, with the comparison of the *in vitro* anti-tumor activity for free DOX, the DOX-loaded ACCL micelles, the DOX-loaded ACCL-FA micelles and the DOX-loaded folate-conjugated acid-insensitive cross-linked (CCL-FA) micelles, it could be found that the DOX-loaded ACCL-FA micelles exhibited higher inhibition of the proliferation of KB cells. In addition, these FA-decorated ACCL micelles showed higher cellular uptake than those micelles without FA moiety, indicating their unique targeted capability. These folate-conjugated core cross-linked biodegradable micelles are highly promising for targeted cancer chemotherapy.

Introduction

Polymeric micelles, self-assembled from amphiphilic block copolymers in aqueous medium with a mesoscopic size range, have been regarded as one of the most commonly used anti-cancer drug delivery systems due to their unique physical and biochemical advantages.[1-4] Biocompatible polymeric micelles have appeared for targeted and controlled delivery of hydrophobic anti-cancer drugs, such as paclitaxel (PTX),[5-7] doxorubicin (DOX),[8] and camptothecin (CPT).[9] These drug-loaded nanoparticles have several advantages, for example, enhancing water solubility of anti-cancer drugs, prolonging drug circulation time, targeting to the tumor tissues *via* the enhanced permeability and retention (EPR) effect, improving drug bioavailability, and decreasing side effects.[10,11] In recent years, several micellar anti-tumor drug devices, such as Genexol-PM,[7] NK-911,[8] NK-105,[12] NK-012,[13] NC-6004,[14,15] NC-4016,[16] BIND-014,[17] have already been approved for different phases of clinical trials.

The applications of polymeric micelles, however, have been hampered because of the poor *in vivo* stability, the large volume dilution and the interactions with blood pool upon administration to systemic circulation. The micellar disintegration in blood before reaching the tumor tissues may result in premature release of encapsulated drugs, reduced therapeutic efficacy and undesired side effects.[18,19] Recent interests in preventing their dissociation have focused on increasing the stability of polymeric micelles. One of the effective strategies is to develop the cross-linking micelles, which can take place on the hydrophilic shells,[20-23] within the hydrophobic cores,[6,24-30] or at the core-shell interfaces.[31,32] The choice of the cross-linking agents is also important because they directly affect the stability and properties of the final cross-linked micelles. With rapid development of the "smart" materials, stimuli-responsive molecules that respond to external triggers such as redox conditions or changes in pH values have attracted increasing attentions. Considering the different pH environments at the internal and external tumor tissues (*e.g.* the pH value of extracellular tumors is 6.5-7.2, while it drops to a lower pH of 5.5-6.0 in endosomes and approaches pH 4.5-5.0 in lysosomes),[33,34] researchers have designed some pH-responsive cross-linking agents for triggered drug delivery system. The hydrolysis of acid-labile groups in the acidic environment of cancer cells would accelerate the dissociation of the drug-loaded micelles and further result in a rapid release of encapsulated drugs.[26,35,36] Therefore, it will be highly beneficial to those anticancer drug delivery systems that keep stable during circulation but are sensitive to the signal caused by disease and release proper amount of drugs in response.

Polyphosphoester (PPE)-based materials have great potential applications due to their adjustable properties, facile functionalization, as well as favorable biodegradability and biocompatibility.[37,38] In the backbone of PPEs, there are many repeating phosphoester linkages, allowing to introduce various

functional groups.[39-42] The physical and chemical properties of PPEs can be tuned by varying the pendant side-chain structures. As reported, PPEs have a similar structure with teichoic acid and nucleic acid, and exhibit favorable biocompatibility. In addition, PPEs are prone to degradation through the hydrolysis of the ester bonds under acidic or basic conditions.[43,44] Phosphodiesterase I (PDE I) existed in the cytosomes or subcellular regions of human cells can accelerate the degradation of PPEs.[37,44,45] Traditionally, PPEs were synthesized mainly by polycondensation, polyaddition, transesterification, and ring-opening polymerization (ROP).[37] Since the 1980s, several researchers have explored the biomedical applications of PPEs, initially for controlled drug delivery.[46,47] Subsequently, various kinds of anticancer drug delivery devices based on PPEs have been constructed and examined, such as micelles,[39,48-51] polymeric prodrugs,[40,44,52] nanogels or hydrogels.[53-56]

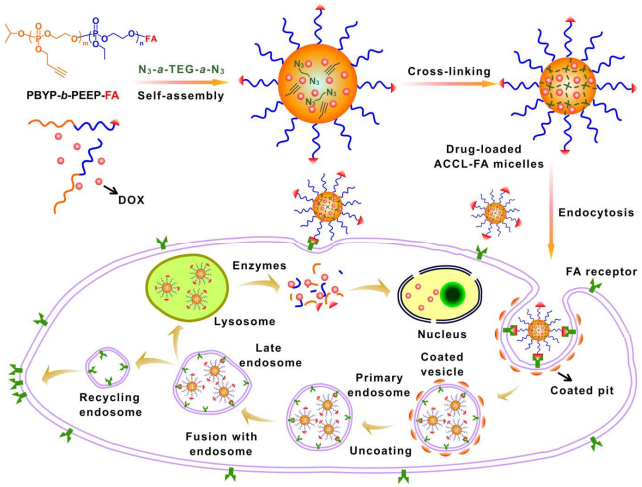

Scheme 1 Illustration of folate-conjugated and core cross-linked polyphosphoester micelles for efficient intracellular release of hydrophobic anticancer drugs triggered by enzymes and acidic microenvironment inside the tumor tissue.

In the present study, we first prepared folate-conjugated amphiphilic block copolymers comprising biodegradable polyphosphoesters, designated as PBYP-*b*-PEEP-FA. As shown in Scheme 1, the diblock polyphosphoesters and a cross-linking agent azide-modified tetraethylene glycol (N_3-*a*-TEG-*a*-N_3) self-assembled into micelles in aqueous solution, which could simultaneously encapsulate the hydrophobic anticancer drug doxorubicin (DOX). Then, the core cross-linking was occurred inside the micellar core *via* a Cu(I)-catalyzed azide-alkyne cycloaddition (CuAAC) "Click" reaction between the azide groups on the acid-cleavable N_3-*a*-TEG-*a*-N_3 and the alkynyl groups on the polyphosphoesters (PBYP-*b*-PEEP or PBYP-*b*-PEEP-FA), endowing the stability of polymeric micelles and effectively preventing premature drug release during the following injection. As folic acid (FA) has been widely exploited for tumor-targeting, the DOX-loaded ACCL-FA micelles would be effectively internalized into FA receptor-overexpressing cancer cells. The acetal linkages in the cross-linker could be cleaved under endosomal and lysosomal acidic conditions once the DOX-loaded micelles were internalized into cancer cells. Both of the cleavage of the cross-linker in acidic environment and the degradation of PPEs in the present of PDE I would lead to the micellar dissociation and subsequent fast drug release. Therefore, this work presents a facile way to prepare novel acid-cleavable core cross-linked micelles based on biodegradable polyphosphoesters, which have great potential in the targeted and triggered release of hydrophobic anti-cancer drugs.

Experimental

Materials

Isopropyl alcohol (IPA, A.R., Xilong Chemical) was dried over anhydrous $MgSO_4$ for 24 h at room temperature and distilled under reduced pressure before use. 2-Ethoxy-2-oxo-1,3,2-dioxaphospholane (EOP) was prepared as described previously,[57] and distilled under reduced pressure before use. 2-(But-3-yn-1-yloxy)-2-oxo-1,3,2-dioxaphospholane (BYP) was prepared and purified according to the literature method.[41] Dimethylsulfoxide (DMSO, A.R., Sinopharm Chemical Reagent) was dried over CaH_2 and distilled under reduced pressure before use. 1,8-diazabicyclo[5.4.0]-undec-7-ene (DBU, 98%, J&K Chemical), *N*-Hydroxysuccinimide (NHS, 98%, Sigma-Aldrich), 4-dimethylamino pyridine (DMAP, 99%, Shanghai Medpep), *N*,*N*′-dicyclohexy-lcarbodiimide (DCC, 99%, Alfa Aesar), phosphodiesterase I (PDE I, Sigma-Aldrich), folic acid (FA, 97%, Sinopharm Chemical Reagent), tetraethylene glycol (TEG, Sigma-Aldrich), 2-chloroethyl vinyl ether (CEVE, 98%, TCI), pyridinium *p*-toluenesulfonate (PPTS, 98%, Acros), chloroacetyl chloride (98%, Shanghai Jingxi Chemical), sodium azide (NaN_3, 98%, Sinopharm Chemical Reagent), *N*,*N*,*N*′,*N*″,*N*″-pentamethyldiethylenetriamine (PMDETA, 98%, Sigma-Aldrich), ascorbic acid (Sinopharm Chemical Reagent), triethylamine (TEA, A.R., Sinopharm Chemical Reagent), 3-(4,5-dimethylthiazol-2-yl)-2,5-diphenylte-trazolium bromide (MTT, 98%, Sigma-Aldrich), DOX·HCl (99%, Beijing Zhongshuo Pharmaceutical Technology Development) and bisbenzimide Hoechst 33342 trihydrochloride (H 33342, 98%, Sigma-Aldrich) were used as received. Cuprous bromide (CuBr, 95%, Sinopharm Chemical Reagent) was purified by washing for three times in turn with acetone, glacial acetic acid, and ethanol, followed by drying under vacuum at room temperature. Milli-Q water (18.2 MΩ cm^{-1}) was generated using a water purification system (Simplicity UV, Millipore). All the other chemicals were all analytical reagents and used as received unless otherwise mentioned. All cell culture related reagents were purchased from Invitrogen/Life Technologies.

Synthesis of acid-cleavable folate-conjugated core cross-linked micelles

The preparation procedure of the folate-conjugated and core cross-linked micelles with acid-cleavable acetal groups (ACCL-FA) is outlined in Scheme 2. The synthesis routes can be divided into four steps: (1) synthesis of an azide and acetal-functionalizced TEG (N_3-*a*-TEG-*a*-N_3); (2) preparation of a polyphosphoester-based diblock copolymer (PBYP-*b*-PEEP) with the alkynyl groups in the pendants *via* the sequential ROP reaction of BYP and EOP monomers using IPA as the initiator and DBU as the organic catalyst; (3) introduction of an targeted folate group at the chain end of PBYP-*b*-PEEP; and (4) formation

of the ACCL-FA micelles by CuAAC "Click" reaction between N_3-*a*-TEG-*a*-N_3 and PBYP-*b*-PEEP-FA.

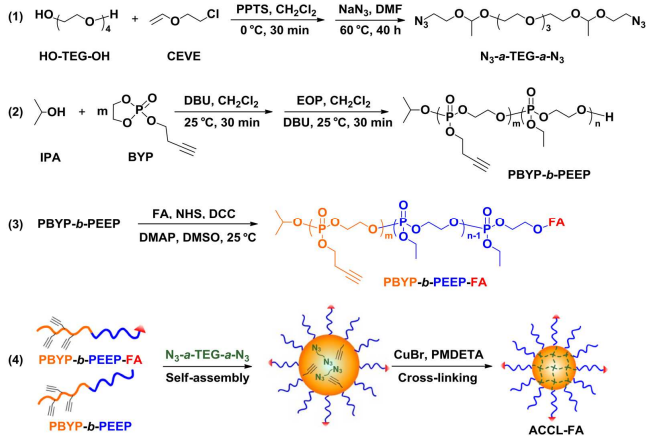

Scheme 2 Synthesis routes of ACCL-FA micelles *via* a combination of ROP and CuAAC "Click" reaction.

Preparation of acid-cleavable cross-linker N_3-*a*-TEG-*a*-N_3

The cross-linker N_3-*a*-TEG-*a*-N_3 was prepared using TEG as a precuror. Typically, TEG (0.97 g, 5 mmol) and PPTS (0.2513 g, 1 mmol) were firstly added into a 50 mL dry flask and purified by azeotropic drying with toluene twice. After 30 mL of anhydrous CH_2Cl_2 was added to dissolve TEG and PPTS, CEVE (2.5 mL, 25 mmol) was added dropwise into the solution at 0 °C under the protection of nitrogen. After stirring for 30 min at 0 °C, the reaction was then quenched by adding 10 mL of 5 wt% Na_2CO_3 aqueous solution. The reaction mixture was diluted with another 30 mL of CH_2Cl_2 and washed with 10 mL of pH buffer solution (pH 10.0), with each aqueous solution being further extracted with 20 mL of CH_2Cl_2. The organic phase was dried over anhydrous $MgSO_4$ for 1 h and evaporated to dryness by rotary evaporation. The residue was purified *via* azeotropic distillation with toluene twice to remove unreacted CEVE, and dried under vacuum to a constant weight (Cl-*a*-TEG-*a*-Cl, 1.1256 g, yield: 74.9%). ^{1}H NMR (400 MHz, $CDCl_3$, ppm): δ 1.34 (d, 6H, −CH(C***H***$_3$)−), δ 3.65 (t, 16H, −OC***H***$_2$C***H***$_2$O−), δ 3.75 (t, 4H, −C***H***$_2$Cl), δ 3.85 (t, 4H, −C***H***$_2$CH$_2$Cl), δ 4.83 (m, 2H, −C***H***(CH$_3$)−).

Cl-*a*-TEG-*a*-Cl (1.025 g, 2.5 mmol) and NaN_3 (1.625 g, 25 mmol) were dissolved in 10 mL of DMF in a 50 mL flask, and the reaction mixture was stirred at 60 °C for 40 h. After removing the insoluble salt by filtration, the filtrate was concentrated under reduced pressure, diluted with 100 mL of CH_2Cl_2, and washed with 10 mL of pH buffer solution (pH 10.0), with each aqueous layer being further extracted with 20 mL of CH_2Cl_2 twice. The organic phase was dried over anhydrous $MgSO_4$ for 1 h, and the filtrate was evaporated by rotary evaporation. The residue was purified by silica gel column chromatography using ethyl acetate as the eluent, and dried under vacuum to a constant weight (N_3-*a*-TEG-*a*-N_3, 0.7581 g, yield: 72.2%). ^{1}H NMR (400 MHz, $CDCl_3$, ppm): δ 1.34 (d, 6H, −CH(C***H***$_3$)−), δ 3.38 (t, 4H, −C***H***$_2$N$_3$), δ 3.65 (t, 16H, −OC***H***$_2$C***H***$_2$O−), δ 3.75 (t, 4H, −C***H***$_2$CH$_2$N$_3$), δ 4.83 (m, 2H, −C***H***(CH$_3$)−). ^{13}C NMR (100 MHz, $CDCl_3$, ppm): δ 19.37 (−CH(***C***H$_3$)−), δ 50.86 (−***C***H$_2$N$_3$), δ 63.73 (−***C***H$_2$OCH−), δ 70.54 (−***C***H$_2$O***C***H$_2$***C***H$_2$O***C***H$_2$−), δ 99.76 (−***C***H(CH$_3$)−). LC/MS *m*/*z* calcd. for $C_{16}H_{32}N_6O_7Na$ $[M{\cdot}Na]^+$: 443.2, found: 443.3.

Preparation of PBYP-*b*-PEEP diblock copolymer

The PBYP-*b*-PEEP diblock copolymer was prepared by the sequential ROP reaction of BYP and EOP in the presence of IPA, using DBU as the catalyst under nitrogen atmosphere. Briefly, a 50 mL dry flask was charged with DBU (0.2738 g, 0.18 mmol) and 1.5 mL of anhydrous CH_2Cl_2 under a nitrogen atmosphere, three exhausting-refilling nitrogen cycles were then taken to degas the solution. To this solution, IPA (0.1121 g, 0.12 mmol) and BYP (0.8453 g, 4.8 mmol) were added under nitrogen atmosphere by a syringe, and the reaction mixture was kept stirring at 25 °C for 30 min. Subsequently, EOP (0.73 g, 4.8 mmol) was injected into the flask by a syringe, and the solution was further stirred at 25 °C for another 30 min. The solvent was removed by rotary evaporation. The product was precipitated in 100 mL of cold methanol/diethyl ether (1/10, *v*/*v*) twice. Afterwards, the mixture was purified by dialysis (MWCO 3500) against Milli-Q water for 24 h. The product was obtained after lyophilization (PBYP-*b*-PEEP, 1.3719 g, yield: 81.3%). ^{1}H NMR (400 MHz, $CDCl_3$, ppm): δ 1.31-1.44 (m, 129H, −CH$_2$C***H***$_3$, −CH(C***H***$_3$)$_2$), δ 2.04-2.17 (s, 43H, ≡C***H***), δ 2.56-2.67 (t, 86H, −C***H***$_2$C≡CH), δ 3.79 (t, 2H, −C***H***$_2$OH), δ 4.10-4.21 (m, 168H, −C***H***$_2$CH$_2$C≡CH, −C***H***$_2$CH$_3$), δ 4.21-4.37 (t, 334H, −OC***H***$_2$C***H***$_2$O−, −OC***H***$_2$CH$_2$OH), δ 4.67 (m, 1H, −C***H***(CH$_3$)$_2$).

Preparation of PBYP-*b*-PEEP-FA

FA (15.9 mg, 0.036 mmol) was dissolved in 10 mL of DMSO under the protection of nitrogen in dark. Then, DCC (9.6 mg, 0.0468 mmol), NHS (5.4 mg, 0.0468 mmol) and DMAP (5.7 mg, 0.0468 mmol) were added into the flask. The mixture was stirred at 25 °C under nitrogen for 12 h. Afterwards, PBYP-*b*-PEEP (0.4161 g, 0.03 mmol) was added, and the mixture was reacted for another 24 h in the same condition. The mixture was dialyzed against Milli-Q water for 24 h using cellulose tubular membrane (MWCO 3500), and then dried by lyophilization. The product was dissolved in CH_2Cl_2 and centrifuged at 5000 rpm for 5 min to remove free FA. Then, the solution was evaporated to dryness by rotary evaporation, and dried under vacuum to a constant weight at room temperature (PBYP-*b*-PEEP-FA, 0.334 g, yield: 77.8%).

Characterizations

^{1}H NMR, ^{13}C NMR, and ^{31}P NMR spectra were recorded on a NMR instrument (INOVA-400) with $CDCl_3$ as the solvent and tetramethylsilane (TMS) as the internal reference. Fourier transform infrared (FT-IR) spectra were performed on a Nicolet 6700 spectrometer using the KBr disk method. The number-average molecular weights and molecular weight distributions (PDIs) of polymers were recorded on a Waters 1515 gel permeation chromatography (GPC) equipped with a Waters 1515 isocratic HPLC pump, a Waters 2414 refractive index detector, a Waters 717 plus autosampler and a set of MZ-Gel SD plus columns (500, 10^3, and 10^4 Å). The measurements were performed using DMF containing 0.05 mol L^{-1} LiBr as the eluent with a flow rate of 0.8 mL min^{-1} at 40 °C. A series of narrowly distributed polystyrene standards were used as the calibration. The UV-Vis absorption spectra were recorded on a UV-Vis spectrophotometer (UV-2550, Shimadzu, Japan). The mass

spectrum was performed on a 1260-6120 LC/MS instrument with methanol as the solvent.

Self-assembly behavior

The critical aggregation concentration (CAC) values were determined by the fluorescence probe method using pyrene as the hydrophobic probe. Typically, a predetermined pyrene solution in acetone was respectively added into a series of ampoules. Acetone was then evaporated and replaced with aqueous polymer solutions at different concentrations in the range from 400 to 8×10^{-3} mg L^{-1}. The final concentration of pyrene in each ampoule was 6×10^{-6} mol L^{-1}. The samples were sonicated for 10 min, stirred at room temperature for 24 h, and analyzed on a spectrofluorometer (FLS920, Edinburgh) at the excitation wavelength of 335 nm and emission wavelength of 350 to 550 nm, with both bandwidths were set at 2 nm. From the pyrene emission spectra, the intensity ratio (I_3/I_1) of the third band (382 nm, I_3) to the first band (371 nm, I_1) was analyzed as a function of polymer concentration. The CAC value was defined as the point of intersection of the two lines in the plot of fluorescence *versus* polymer concentration.

Preparation of acid-cleavable core cross-linked (ACCL) micelles and uncross-linked (UCL) micelles

The ACCL micelles were prepared using the CuAAC "Click" reaction. In brief, $PBYP_{43}$-*b*-$PEEP_{41}$ (10 mg, 0.72 μmol) and N_3-*a*-TEG-*a*-N_3 (6.5 mg, 0.0155 mmol) were dissolved in 2 mL of DMF in a 50 mL round-bottom flask. Then, 20 mL of Milli-Q water was added dropwise under moderate stirring. After vigorous stirring for another 12 h, CuBr (4.4 mg, 0.031 mmol), PMDETA (1.3 μL, 0.062 mmol) and ascorbic acid (5.5 mg, 0.031 mmol) were added into the reaction mixture, followed by three freeze-pump-thaw nitrogen cycles. The reaction mixture was stirred at 25 °C for 24 h. The ACCL micelles were further dialyzed (MWCO 3500) against Milli-Q water for 24 h. The dialysis medium was changed five times during the process. Finally, the ACCL micelle solution was diluted to 25 mL with Milli-Q water to a desired concentration. The targeted ACCL-FA micelles containing folic acid at the surface of micelles were prepared according to the above-mentioned method, using $PBYP_{43}$-*b*-$PEEP_{41}$-FA to react with the acid-sensitive cross-linker N_3-*a*-TEG-*a*-N_3. The acid-insensitive core cross-linked (CCL) micelles were prepared *via* the reaction of $PBYP_{43}$-*b*-$PEEP_{41}$ with the acid-insensitive cross-linker N_3-TEG-N_3.

The UCL micelles were prepared by a dialysis method. In brief, 10 mg of $PBYP_{43}$-*b*-$PEEP_{41}$ was first dissolved in 2 mL of DMF in a 50 mL round-bottom flask. Then, 20 mL of Milli-Q water was added dropwise under moderate stirring. After vigorous stirring for another 12 h at room temperature, the UCL micelles were further dialyzed against Milli-Q water for 24 h to remove DMF (MWCO 3500). The dialysis medium was changed five times during the process. Finally, the UCL micelle solution was diluted to 25 mL with Milli-Q water to a desired concentration. As a control sample, the targeted UCL-FA micelles containing folic acid on the surface of micelles were prepared through the self-assembly of $PBYP_{43}$-*b*-$PEEP_{41}$-FA.

Encapsulation of DOX

DOX-loaded ACCL micelles were prepared by the similar procedure as that for blank ACCL micelles. At first, $PBYP_{43}$-*b*-$PEEP_{41}$ (10 mg, 0.72 μmol) and N_3-*a*-TEG-*a*-N_3 (6.5 mg, 0.0155 mmol) were dissolved in 2 mL of DMF in a 50 mL round-bottomed flask, followed by adding 0.4 mL of DOX solution in DMSO (5 mg mL^{-1}). Then, 20 mL of Milli-Q water was added dropwise under moderate stirring. After vigorous stirring for another 12 h, CuBr (4.4 mg, 0.031 mmol), PMDETA (1.3 μL, 0.062 mmol) and ascorbic acid (5.5 mg, 0.031 mmol) were added into the reaction mixture, followed by three freeze-pump-thaw nitrogen cycles. The reaction mixture was stirred at 25 °C for 24 h. The DOX-loaded ACCL micelles were further dialyzed (MWCO 3500) against Milli-Q water for 24 h at room temperature to remove DMF and free DOX. The dialysis medium was changed five times during the process. Finally, the DOX-loaded micelle solution was diluted to 25 mL with Milli-Q water to a desired concentration. For determining the DOX loading content, 2 mL of the solution was lyophilized and dissolved in 4 mL of DMF. The solution was measured by fluorescence spectroscopy (FLS920, Edinburgh) with excitation at 480 nm and emission at 560 nm, and the slit width was set at 5 nm. The whole procedure was performed in the dark. The drug loading content (DLC) and the drug loading efficiency (DLE) were calculated according to the following equations:

$$\text{DLC}\,(\%) = \frac{\text{Weight of DOX in micelles}}{\text{Weight of polymers}} \times 100 \qquad (1)$$

$$\text{DLE}\,(\%) = \frac{\text{Weight of DOX in micelles}}{\text{Weight of DOX in feed}} \times 100 \qquad (2)$$

For comparison with the DOX-loaded ACCL micelles, we synthesized another DOX-loaded core cross-linked micelles without acetal linkages (CCL). The DOX-loaded CCL micelles were prepared by the same procedure as for the DOX-loaded ACCL micelles. The preparation procedure is described in the ESI in details.

Characterizations of micelles

The average particle sizes ($\bar{D}_z$) and size polydispersity indices (size PDIs) of the polymeric micelles were carried out at 25 °C using a dynamic light scattering instrument (Zetasizer Nano ZS, Malvern) equipped with a 633 nm He-Ne laser and 90° collecting optics using back-scattering detection. Dust particles were removed by filtering each polymer solution through a Φ = 0.45 μm microfilter before measurements.

The morphologies of the polymeric micelles were observed by a transmission electron microscopy (TEM) instrument (Tecnai G^2 20, FEI) operated at an accelerating voltage of 200 kV. All samples were prepared as described in particle size determination, and the samples were then prepared by a freeze-drying method.[58,59] The carbon-coated copper grid was placed on the bottom of a glass cell, which was then immediately inserted into liquid nitrogen. Subsequently, 8 μL of the micellar solution was dripped onto the grid, and the solvent in its frozen solid state was directly removed without melting in a freeze-drier. The morphologies were then imaged on a normal TEM instrument at room temperature.

In vitro DOX release

The release profiles of DOX from drug-loaded micelles were investigated at 37 °C in three different media, the acetate buffer solution (pH 5.0, 10 mM), the phosphate buffer solution (pH 7.4, 10 mM), and the phosphate buffer solution (pH 7.4, 10 mM) with 0.25 mg mL^{-1} PDE I and 5 mg mL^{-1} $MgCl_2 \cdot H_2O$, respectively. Typically, 5 mL of the prepared DOX-loaded solution was transferred into a dialysis membrane bag (MWCO 12000-14000), which was subsequently immersed into a tube containing 20 mL of the corresponding buffer solution. The tube was then put into a shaking water bath at 37 °C. At predetermined intervals, 5 mL of the release medium was taken out and replenished with an equal volume of the corresponding fresh buffer solution. Fluorescence measurement was carried out to determine the concentration of released DOX. All the release experiments were conducted in triplicate with standard deviations in the dark.

In vitro enzymatic degradation

The degradation process was monitored by NMR measurement in a phosphate buffer solution (pH 7.4, 10 mM) at 37 °C with constant gentle shaking. Typically, 30 mg of $PBYP_{43}$-*b*-$PEEP_{41}$ was dissolved in 15 mL of the buffer solution containing 7.5 mg PDE I and 75 mg $MgCl_2 \cdot H_2O$. The solution was then divided into three portions and immersed into a thermostatic shaker at 37 °C. At predetermined time intervals, each solution was taken out and lyophilized for the NMR analysis.

MTT assays

A standard MTT assay was employed to evaluate the cytotoxicity of several polymer micelles. L929 cells were seeded in 96-well plates at a density of about 5×10^4 cells per well and cultured in DMEM culture medium with 10% serum and 1% penicillin/streptomycin in an incubator at 37 °C in 5% CO_2 atmosphere for 24 h. Then, the polymer solutions with different concentrations were added into each well and incubated with the cells for another 48 h. Afterwards, 25 μL of the MTT stock solution (5 mg mL^{-1} in PBS) was added to each well. After incubation for another 4 h, the DMEM medium was removed and 150 μL of DMSO was added to each well. The optical density (OD) at 570 nm of each well was measured on a microplate reader (Bio-Rad 680). The absorbance values were normalized to wells, in which cells were not treated with block copolymers. The data were presented as the average values with standard deviations. In addition, a standard MTT assay was employed to evaluate the cytotoxicity of DOX-loaded nanoparticles against KB cells using free DOX and blank nanoparticles as the controls. RPMI-1640(-)FA culture medium was used to incubate KB cells for at least two weeks to allow the exposure of folate receptor, and the MTT assay experiments were then conducted according to the similar method used for L929 cells.

Intracellular release of DOX

The cellular uptake and intracellular release behaviors of DOX-loaded ACCL-FA and ACCL micelles were monitored with a live cell imaging system (CELL'R, Olympus, Japan) using KB cells. Typically, KB cells were seeded in a Φ = 35 mm glass Petri dish at a density of 5×10^4 cells cm^{-2}, and the dish was located in the incubator of a live cell imaging system at 37 °C under 5% CO_2-containing atmosphere. The culture medium was removed after 12 h of incubation, and the cells were washed with PBS and stained with H 33342 (10 mg L^{-1}) for 15 min. Afterwards, The culture medium was then replaced with RPMI-1640(-)FA medium containing DOX-loaded micelles (0.3 mg L^{-1} of DOX). The images were then captured with an excitation wavelength of 480 nm (red) and 340 nm (blue) for 4 h.

Flow cytometry analysis

KB cells were seeded in 35 mm cell culture dishes at a density of 5×10^4 cells cm^{-2} and allowed to adhere for 12 h. Subsequently, the culture medium was replaced by 1 mL of fresh medium (either with or without FA ligands DOX-loaded CCL micelles, the final concentration of DOX was 0.3 mg L^{-1}). After incubation at 37 °C for different times, the culture medium was removed, and the cells were then washed with PBS three times and digested with trypsin. Afterwards, 2 mL of culture medium was added to each culture dish, and the solutions were centrifuged for 3 min at 1000 rpm. After removed the supernatants, the cells were resuspended in 0.5 mL of PBS. The fluorescence histograms of DOX in cells were recorded using flow cytometry (Cytomics FC500, Beckman Coulter, American).

Results and discussion

Characterizations

As illustrated in the first step in Scheme 2, the acid-cleavable cross-linker N_3-*a*-TEG-*a*-N_3 was prepared *via* an acetalation and a nucleophilic substitution reaction. Figure S1 shows the ^1H NMR spectra of the acid-cleavable precursor Cl-*a*-TEG-*a*-Cl (Figure S1(A)) and N_3-*a*-TEG-*a*-N_3 (Figure S1(B)). As shown in Figure S1(A), all of the characteristic signals (peaks a) of methylene protons assigned to TEG can be found. Also, the new resonances appeared at δ 1.34 ppm (peak c), δ 3.75 ppm (peak e), δ 3.85 ppm (peak d), and δ 4.83 ppm (peak b), which can be attributed to the protons of methyl (−CH(C***H***$_3$)−), methylene (−C***H***$_2$C***H***$_2$Cl), and acetal methine (−C***H***(CH$_3$)−), respectively. The clickable N_3-*a*-TEG-*a*-N_3 was synthesized by a nucleophilic substitution reaction between Cl-*a*-TEG-*a*-Cl and NaN_3. With the comparison of the integral area of corresponding peaks, it is notable that the resonance at δ 3.75 ppm attributed to the methylene protons (−CH_2C***H***$_2$Cl) disappeared completely. A new signal at δ 3.38 ppm assigned to the methylene protons (−CH_2C***H***$_2$$N_3$) appeared in Figure S1(B), which confirm the successful synthesis of clickable cross-linking agent N_3-*a*-TEG-*a*-N_3. Similarly, as evidenced from the ^{13}C NMR spectrum shown in Figure S2, resonances of carbon atoms assigned to N_3-*a*-TEG-*a*-N_3 are all presented. Moreover, FT-IR measurements were also carried out to further demonstrate the successful preparation of N_3-*a*-TEG-*a*-N_3. Figure S3(A)~(C) display the FT-IR spectra of TEG, Cl-*a*-TEG-*a*-Cl, and N_3-*a*-TEG-*a*-N_3, respectively. It is clearly observed that the original absorption peak at 3383 cm^{-1} in Figure S3(A) corresponding to hydroxyl groups of TEG disappeared in Figure S3(B) after the addition reaction. The FT-IR spectrum of N_3-*a*-TEG-*a*-N_3 shows a new absorption peak at 2106 cm^{-1} corresponding to azide groups in Figure S3(C), indicating the successful formation of N_3-*a*-TEG-*a*-N_3.

As a comparison, diazide-functionalized TEG (N_3-TEG-N_3) without the acid-cleavable acetal linkage was synthesized *via* an

esterification reaction between TEG and chloroacetyl chloride, followed by nucleophilic substitution reaction with NaN_3. The preparation procedure of N_3-TEG-N_3 is depicted in Scheme S1. The chemical structure of N_3-TEG-N_3 was verified by ^{1}H NMR, ^{13}C NMR and FT-IR analyses, as shown in Figure S4, S5 and S6, respectively.

The well-defined diblock polyphosphoester PBYP-*b*-PEEP was prepared *via* one-pot sequential ROP reaction, which we found here is more efficient than the other chain-extension way from purified macroinitiators. ^{31}P NMR, ^{1}H NMR, and GPC measurements were carried out to characterize the chemical structure, molecular weights, and molecular weight distributions of the copolymers. The conversion of BYP was estimated from ^{31}P NMR spectrum by comparing the integral ratio of two distinct peaks of BYP monomer and PBYP homopolymer. Figure S7(A) displays the ^{31}P NMR spectrum of the reaction mixture of PBYP without purification. The peaks at δ -1.81 ppm and δ 17.63 ppm are the characteristic signals of PBYP and BYP, respectively. The conversion of BYP could be reached more than 95% in 30 min. The reactant was purified by precipitation from CH_2Cl_2 into a mixture of cold methanol/diethyl ether (1/10, *v*/*v*) twice, followed by dialysis (MWCO 3500) against Milli-Q water/ethanol mixture (2/1, *v*/*v*) for 24 h. The ^{1}H NMR spectrum of $PBYP_{43}$ is shown in Figure 1(A). The resonances appeared at δ 2.04-2.17 ppm (peak l), δ 2.56-2.67 ppm (peak k), δ 3.79 ppm (peak i), δ 4.10-4.21 ppm (peak j), and δ 4.21-4.37 ppm (peak h) can be attributed to the protons of alkynyl group (≡C***H***), methylene beside the alkynyl group (−C***H***$_2$C≡CH), methylene at the chain end (−C***H***$_2$OH), methylene in the side chain (−C***H***$_2$CH$_2$C≡CH), and methylene in the backbone (−OC***H***$_2$C***H***$_2$O−, −OC***H***$_2$CH$_2$OH), respectively. Furthermore, some characteristic resonance signals can be observed at δ 1.36 ppm (peak f) and δ 4.67 ppm (peak g) that are attributed to the protons of IPA.

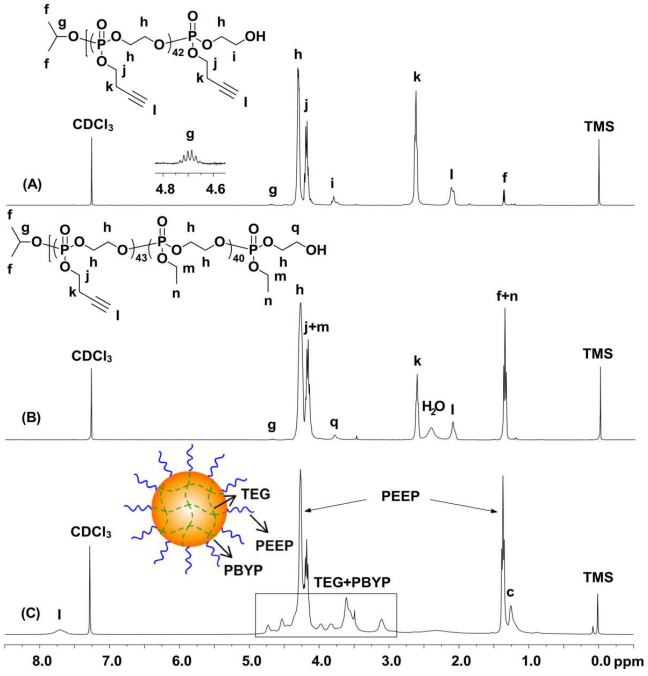

Figure 1 ^{1}H NMR spectra of (A) $PBYP_{43}$, (B) $PBYP_{43}$-*b*-$PEEP_{41}$, and (C) lyophilized ACCL micelles in $CDCl_3$.

The chemical structure of $PBYP_{43}$-*b*-$PEEP_{41}$ was confirmed by ^{31}P NMR spectrum in Figure S7(B) and ^{1}H NMR spectrum in Figure 1(B). The ^{31}P NMR spectrum of $PBYP_{43}$-*b*-$PEEP_{41}$ displays three signals at δ -1.80, -1.44 and -0.77 ppm that are assigned to the three kinds of phosphorus atoms in PBYP block, PEEP block and the repeat unit at the PEEP chain end, respectively. As shown in Figure 1(B), the resonance signals attributed to protons of PBYP segments can be clearly observed. Furthermore, some characteristic resonance signals noted at δ 1.31-1.44, 4.10-4.21, and 4.21-4.37 ppm become stronger, which can be attributed to the protons of the PEEP block.

Table 1. Characterization data of the compositions, the number-average molecular weights and the molecular weight distributions (PDIs) of various polymers.

Polymers	$\overline{M}_{n,\,theor.}$ [a] (g mol^{-1})	$\overline{M}_{n,\,NMR}$ [b] (g mol^{-1})	$\overline{M}_{n,\,GPC}$ [c] (g mol^{-1})	PDI[c]
$PBYP_{43}$	7100	7630	8920	1.17
$PBYP_{43}$-*b*-$PEEP_{41}$	13190	13870	12590	1.29
$PBYP_{28}$-*b*-$PEEP_{48}$	9610	12230	11070	1.30

[a] As determined in theory. [b] As calculated from ^{1}H NMR spectra in $CDCl_3$. [c] As measured by GPC with DMF as the eluent, using polystyrene as the standards.

Table 1 summarizes the chemical compositions, the number-average molecular weights ($\overline{M}_{n,\,NMR}$) and the molecular weight distributions (PDIs) of various polymers used in the present study. Based on the ^{1}H NMR spectra of Figure 1, the molecular weights ($\overline{M}_{n,\,NMR}$) of PBYP and PBYP-*b*-PEEP were calculated according to eqn. (3) and (4), respectively:

$$\overline{M}_{n,\,NMR\,(PBYP)} = \frac{3A_k}{A_f} \times 176.02 + 60 \qquad (3)$$

$$\overline{M}_{n,\,NMR\,(PBYP\text{-}b\text{-}PEEP)} = \left(\frac{2A_{f+n}}{3A_k} \times DP_{PBYP} - 2\right) \times 152.02 + \overline{M}_{n,\,NMR\,(PBYP)} \qquad (4)$$

where A_k and A_f are the integral values of the peaks k and f in Figure 1(A), respectively; A_{f+n} is the integral value of the peak (f+n) in Figure 1(B); 176.02 is the molecular weight of one repeating unit of PBYP; 60 is the molecular weight of the IPA molecular, and 152.02 is the molecular weight of one repeating unit of the PEEP block; DP_{PBYP} and $\overline{M}_{n,\,NMR\,(PBYP)}$ are the degree of polymerization and molecular weight of the PBYP homopolymer, respectively.

The chemical structure of $PBYP_{43}$-*b*-$PEEP_{41}$-FA was confirmed by UV-Vis analysis. As shown in Figure S8, in the wavelength range from 400 to 220 nm, the maximum absorption peak of free FA is at 283 nm, while $PBYP_{43}$-*b*-$PEEP_{41}$ rarely has any UV absorption in this range. Therefore, the maximum absorption peak at about 277 nm could be attributed to $PBYP_{43}$-*b*-$PEEP_{41}$-FA, and further confirmed the successful conjugation of $PBYP_{43}$-*b*-$PEEP_{41}$ with FA. In addition, the blue shift occurred for $PBYP_{43}$-*b*-$PEEP_{41}$-FA may be attributed to the covalent linkage of FA to $PBYP_{43}$-*b*-$PEEP_{41}$ by one of the carboxyl groups of FA. Moreover, the FA content was calculated according to eqn. (5), where $C_{UV\text{-}Vis}$ represents the concentration of FA measured by UV-Vis, and $C_{PBYP\text{-}b\text{-}PEEP\text{-}FA}$ is the concentration of the FA-

contained polymer. In this study, the FA content of $PBYP_{43}$-*b*-$PEEP_{41}$-FA was calculated to be 0.46 wt% (14.45 mol%).

$$C_{FA}(wt\%) = \frac{C_{UV\text{-}Vis}}{C_{PBYP\text{-}b\text{-}PEEP\text{-}FA}} \times 100 \qquad (5)$$

Micellization of block copolymers and core cross-linking

In the present work, we have prepared three kinds of micelles from $PBYP_{43}$-*b*-$PEEP_{41}$, that is, the uncross-linked (UCL) micelles, the acid-insensitive core cross-linked (CCL) micelles using N_3-TEG-N_3 as the cross-linker, and the acid-cleavable core cross-linked (ACCL) micelles using N_3-*a*-TEG-*a*-N_3 as the cross-linker, respectively. The critical aggregation concentration (CAC) value of the $PBYP_{43}$-*b*-$PEEP_{41}$ copolymer was determined by the steady-state fluorescence probe method using pyrene as the probe, which can be an indicative of thermodynamic stability of micelles in aqueous medium. Figure S9 shows the relationship of I_3/I_1 as a function of the logarithm concentrations of copolymer, from which the CAC value (14.1 mg L^{-1}) of $PBYP_{43}$-*b*-$PEEP_{41}$ is determined by intersecting the two straight lines.

The morphology, average particle sizes ($\bar{D}_z$) and size polydispersity indices (size PDIs) of the nanoparticles self-assembled from various copolymers were investigated by TEM and DLS measurements. Figure 2(A, B) and 2(G, H) exhibit the TEM images of the UCL and ACCL nanoparticles self-assembled from $PBYP_{43}$-*b*-$PEEP_{41}$, from which we can find that these copolymers mainly form spherical micelles and are well dispersed in aqueous solution. The decrease in size for the ACCL micelles can be attributed to the formation of new covalent bonds and packing inside the core. In addition, the corresponding size distribution curves of the polymeric micelles measured by DLS display the monomodal peaks as shown in Figure 2(C) and 2(I). The average particle sizes observed by TEM are a little smaller than those obtained from DLS. This is most likely due to the shrinkage of the hydrophilic PEEP shell in TEM analysis while they can be extended into water phase in DLS measurement.

TEM and DLS measurements were performed to further verify the success of core cross-linking. The solution with a concentration of 400 mg L^{-1} was prepared by directly dissolving the UCL and ACCL polymers in methanol, and stirred for one day before use. Figure 2(D, E) exhibits the TEM images of the UCL micelles obtained by directly dissolving diblock copolymers in methanol, from which we can find that these copolymers completely dissolved in solvent. Also, the corresponding size distribution curve measured by DLS in Figure 2(F) displays monomodal peak and completely dissociated into unimers. However, the ACCL micelles in Figure 2(J, K) were not dissolved in methanol under the same conditions. The average particle size of the ACCL micelles was larger in methanol than in aqueous solution, which was mainly due to the penetration of solvent to allow the swelling of the cross-linked micellar core.[6,27]

^{1}H NMR measurement was used to demonstrate the CuAAC "Click" reaction between N_3-*a*-TEG-*a*-N_3 and $PBYP_{43}$-*b*-$PEEP_{41}$. $CDCl_3$ is a good solvent for N_3-*a*-TEG-*a*-N_3 and the diblock copolymer PBYP-*b*-PEEP. After the core cross-linking reaction, these two segments could not be dissolved in $CDCl_3$. Figure 1(C) shows the ^{1}H NMR spectrum of the ACCL micelles, from which one can find that the original signals ascribed to the protons of TEG (Figure 1(A)) and PBYP (Figure 1(B)) become weaker, while the peak of PEEP is still maintained, confirming the formation of ACCL micelles in $CDCl_3$. As the PBYP segment is present in the core, the formed covalent bonds among the PBYP segments result in the rigidity of the hydrophobic core to maintain the micellar structure in organic solvents. In addition, the solvent is unable to penetrate the interior of the core, the signal corresponding to the intensity of the PBYP block at the interior was weakened. In the FT-IR spectrum as shown in Figure S3(E) the absorption peak at 2106 cm^{-1} attributed to the azide group completely disappeared after the "Click" reaction, indicating that the CuAAC "Click" reaction has been successfully achieved.

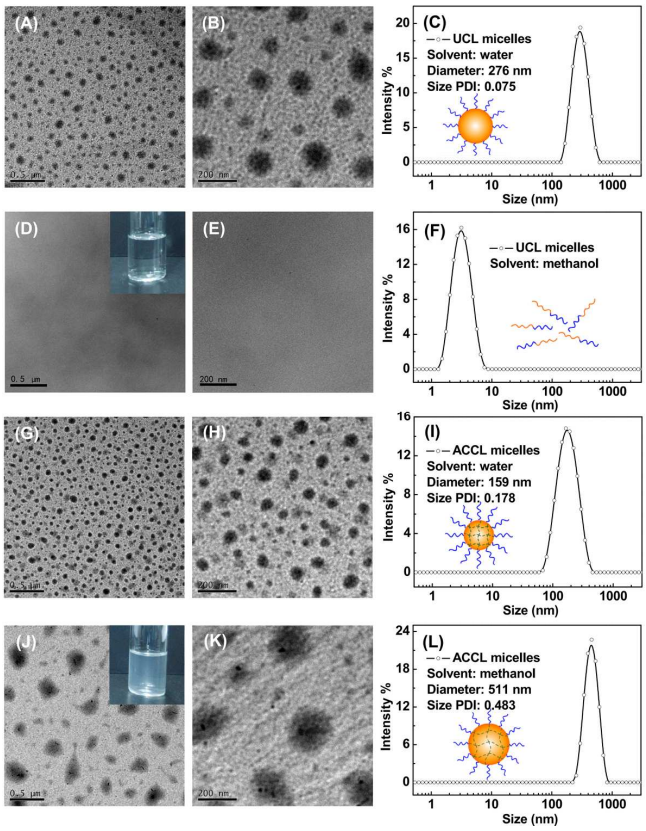

Figure 2 TEM images marked separately by two bars (0.5 μm and 200 nm): (A) and (B) the UCL micelles in Milli-Q water; (D) and (E) the UCL micelles in methanol; (G) and (H) the ACCL micelles in Milli-Q water; (J) and (K) the ACCL micelles in methanol. (C), (F), (I), and (L) the particle size distribution curves corresponding to the samples in (A, B), (D, E), (G, H), and (J, K), respectively. The polymer concentrations were kept at 400 mg L^{-1}.

In vitro DOX encapsulation and release

The hydrophobic anticancer drug DOX was encapsulated into micelles by a dialysis method. Table 2 summerizes the particle sizes ($\bar{D}_z$), the size polydispersity indexes (size PDIs), the drug loading content (DLC) and the drug loading efficiency (DLE) of various DOX-loaded micelles. In this study, the theoretical DLC values were set to 20 wt%. For the ACCL micelles, the actual DLC and DLE values were measured as 11.4% and 57.2%, respectively, which were much higher than those of the uncross-linked micelles (UCL). This can be attributed to the improved stability of the drug-loaded micelles after cross-linking. The DLS results showed that the size of the DOX-loaded ACCL micelles

was smaller than 200 nm. Figure 3(A) shows the TEM image of the DOX-loaded ACCL micelles in aqueous solution, from which one can find that these DOX-loaded micelles mainly form spherical micelles.

Table 2 Micelle sizes ($\bar{D}_z$), size PDIs, DLC and DLE values of DOX-loaded micelles.

Samples	Size[a] (nm)	Size PDIs[a]	Theor. DLC (wt%)	DLC[b] (wt%)	DLE[b] (wt%)
ACCL	166 ± 1	0.144	20	11.4	57.2
UCL	358 ± 10	0.244	20	5.0	25.2

[a] Determined by DLS measurement. [b] Determined by fluorescence measurement.

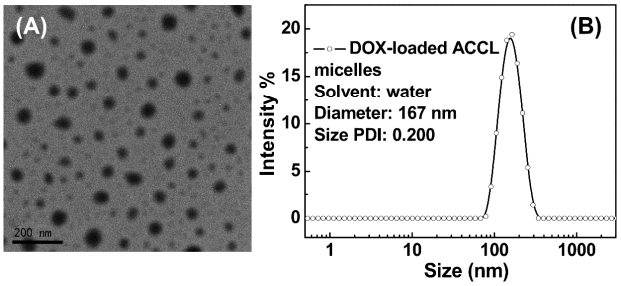

Figure 3 (A) TEM image of the DOX-loaded ACCL micelles (Scale bar = 200 nm) and (B) the particle size distribution curve corresponding to the TEM sample.

pH-responsive polymers are very important in biomedical applications and they are frequently used in triggered drug delivery systems as pH values in different tissues and cellular compartments vary tremendously. In this study, the acetal groups in the cross-linker make the drug carrier susceptible to be degraded in acidic media, which ensures the drug-loaded micelles stable at physiological condition and release DOX in the cytoplasm and/or right into the cell nucleus. To investigate the effects of various media on the release behavior of these nanoparticles, a series of *in vitro* cumulative DOX release data were measured in three different media: (i) pH 5.0, (ii) pH 7.4, and (iii) pH 7.4 with 0.25 mg mL^{-1} of PDE I and 5 mg mL^{-1} of $MgCl_2{\cdot}H_2O$, as shown in Figure 4. Interestingly, approximately 30% of DOX was released from the UCL micelles in 72 h, whereas the release of drugs was significantly inhibited and only approximately 20% of drug was released from the DOX-loaded ACCL and the CCL micelles under the same condition, which is in good agreement with their high stability as shown previously. The drug release rate at pH 5.0 was much faster than that at pH 7.4 for the ACCL, CCL and UCL micelles. This pH-sensitive release behavior can be considered as the partial hydrolysis of polyphosphoester at acidic condition. In addition, the drug release rate for the ACCL micelles was much faster than the CCL micelles at pH 5.0 under the same condition, which was due to the scission of the acetal linkages at acidic condition. Normally, PDE I existing in tumor cells would accelerate the degradation of polyphosphoesters. We have checked the release rate of the DOX-loaded ACCL, CCL, and UCL micelles in the presence of PDE I, and found that the drug release rate was higher than that in absence of PDE I.

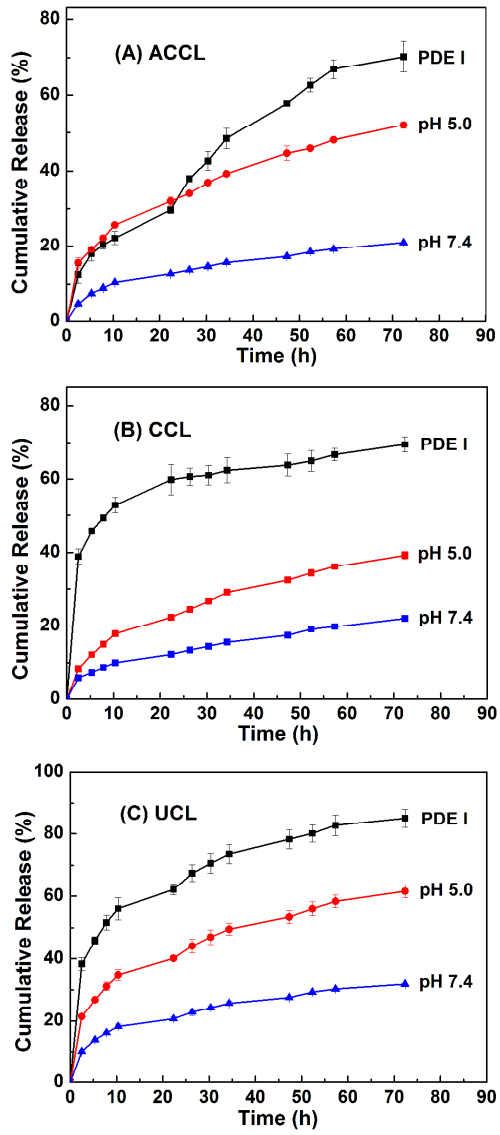

Figure 4 *In vitro* DOX release cures for (A) ACCL, (B) CCL and (C) UCL micelles at 37 °C under different conditions: the pH 5.0 buffer solution, the pH 7.4 buffer solution, and the pH 7.4 buffer solution with PDE I. The micelles concentrations were 400 mg L^{-1}.

Enzymatic degradation

The *in vitro* degradation behavior of the PBYP-*b*-PEEP diblock copolymer was investigated at 37 °C at neutral pH in the presence of PDE I. The degradation time were conducted for 24, 48 and 72 h, respectively, and then taken out to lyophilize for ^{1}H NMR analysis. Figure 5 shows the ^{1}H NMR spectra of $PBYP_{43}$-*b*-$PEEP_{41}$ and its degradation products at different degradation time. These results showed that the original signals assigned to protons of the PBYP and PEEP blocks disappeared gradually, and new signals appeared at δ 0.85, 1.28 and 1.58 ppm, indicating that PBYP-*b*-PEEP possesses good biodegradability in the presence of PDE I.

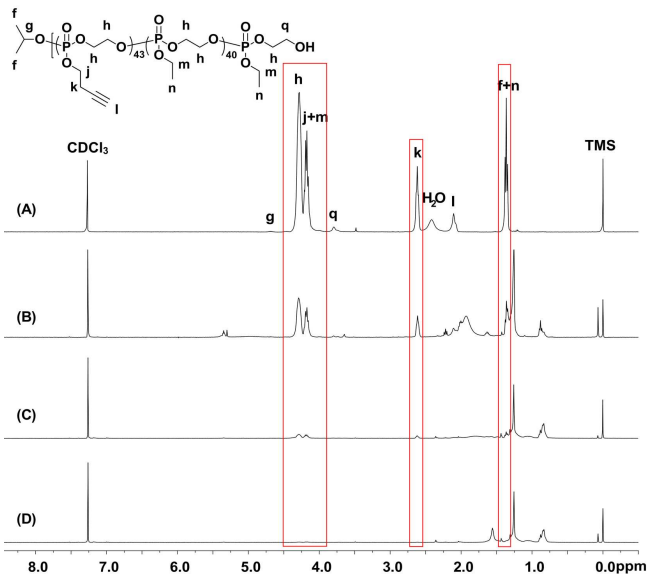

Figure 5 ^{1}H NMR spectra of (A) the $PBYP_{43}$-*b*-$PEEP_{41}$ diblock copolymer and its degradation products after different degradation time for (B) 24 h, (C) 48 h, and (D) 72 h, respectively, measured in $CDCl_3$.

In vitro cytotoxicity

Biocompatibility is one of the most important properties to be considered in selecting biomedical materials. Herein, the cytotoxicity of the FA-containing acid-cleavable core cross-linked (ACCL-FA) micelles and the FA-containing uncross-linked (UCL-FA) micelles against L929 cells and KB cells was studied by the MTT assays. As shown in Figure 6, all blank micelles exhibited minimal cytotoxicity against L929 cells and KB cells with polymer concentrations up to 200 mg L^{-1}, implying the low cytotoxicity of these polymeric micelles.

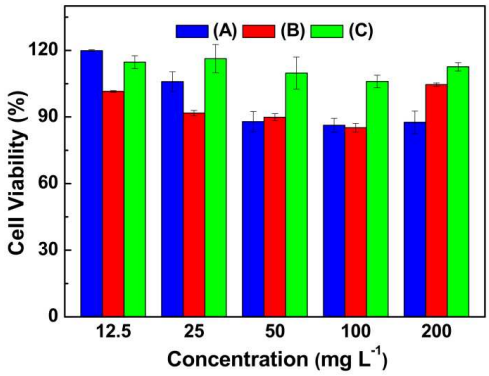

Figure 6 Cell viability of L929 fibroblast cells incubated with (A) the UCL-FA micelles and (B) the ACCL-FA micelles at different concentrations; and (C) cell viability of KB cells incubated with the ACCL-FA micelles at different concentrations. All the incubation time was 48 h.

The targetability of FA-decorated DOX-loaded micelles was evaluated using KB cells because KB cells possess overexpressed folate receptors. KB cells were cultured in RPMI-1640(-)FA medium and treated with the DOX-loaded micelles and free DOX for 48 h. The cell viability was assessed by the MTT assays. The results in Figure 7 show that the viabilities of KB cells were decreased with increasing DOX concentrations. The IC_{50} values, representing DOX dosage for inhibitory concentration to produce 50% cell death, were different for the various nanoparticles, for example, about 0.76 (ACCL-FA), 0.92 (ACCL), 0.92 (CCL-FA), and 2.31 mg L^{-1} (free DOX), respectively, indicating that the DOX-loaded micelles exhibited higher inhibition to the KB cell proliferation after 48 h of culture in comparison with free DOX. It is conceivable that the DOX-loaded micelles are internalized into KB cells *via* an endocytosis mechanism, while free DOX entered into the cells by a passive diffusion process. Therefore, free DOX can enter into cells fast at first, but is then pumped out of the cells quickly.[60-62] The higher anti-tumor activity of the DOX-loaded ACCL-FA system relative to the DOX-loaded ACCL nanoparticles indicated that DOX could be more efficiently delivered and released into the KB cells owing to FA-mediated endocytosis. In addition, the DOX-loaded ACCL-FA nanoparticles with acetal groups exhibited higher anti-tumor activity than the DOX-loaded CCL-FA nanoparticles without acetal groups, which can be ascribed to the scission of the acetal linkages at the junction between cross-linker and backbone segments.

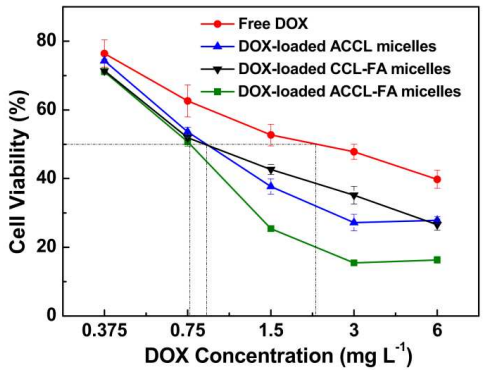

Figure 7 Cell viability of KB cells after incubation for 48 h with free DOX and various DOX-loaded micelles as a function of DOX concentrations.

Intracellular release of DOX

The cellular uptake and intracellular drug release behaviors of the DOX-loaded micelles with or without targeted folic acid, that is, ACCL-FA or ACCL, were monitored using a live cell imaging system, which could synchronously record the dynamic uptake process and the variation of fluorescence intensity inside the KB cells. The cell nuclei were stained with H 33342 (blue). As shown in Figure 8, the DOX fluorescence was observed in KB cells after incubated with the DOX-loaded ACCL-FA micelles for 0.5 h, indicating the fast internalization of the DOX-loaded micelles and the efficient release of DOX inside cells. The red fluorescence intensity of DOX with a gradual increase can be observed with the increase of incubation time. These results indicated that the DOX-loaded ACCL-FA micelles could be internalized into KB cells within several hours, and this is significant for applications as promising drug carriers. In contrast, for the DOX-loaded ACCL micelles without FA, the DOX fluorescence in KB cells is weaker than that of the system containing FA after being incubated for 4 h, indicating that only small amount of the DOX-loaded ACCL micelles was internalized by KB cells.

Flow cytometry analysis further demonstrated the FA-mediated endocytosis process. Figure 9 evidently reveals that the relative geometrical mean fluorescence intensities (GMFI) of the

internalized DOX-loaded ACCL-FA micelles by KB cells increased with the incubation time. In particular, the results showed that the FA-decorated micelles had significantly higher cellular uptake (~1.9 fold) at 2 h incubation than those without FA, indicating that FA greatly improved the specific cell binding and cellular uptake of the DOX-loaded nanoparticles by FA receptor-overexpressing KB cells.

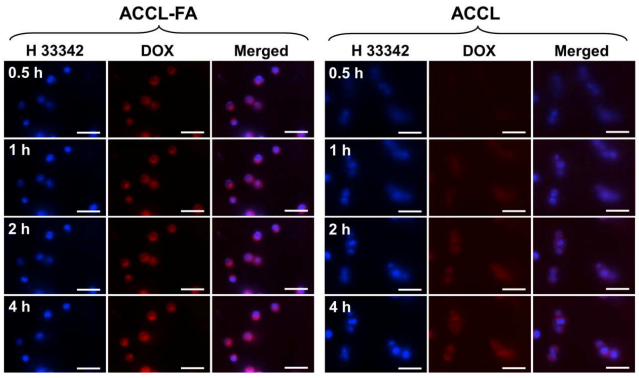

Figure 8 Live cell imaging system images of KB cells incubated with the DOX-loaded ACCL-FA and ACCL micelles (DOX dosage was 0.3 mg L^{-1}) for different time. For each panel, images from left to right show the cell nuclei stained by H 33342 (blue), the DOX fluorescence in cells (red), and overlays of the two images. The scale bars are 50 μm in all images.

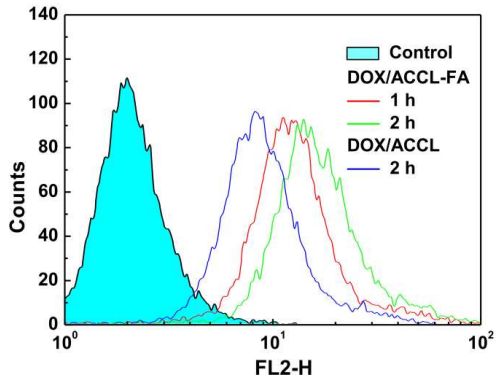

Figure 9 Flow cytometry histogram profiles of KB cells incubated with the DOX-loaded ACCL-FA and ACCL micelles for different time. The dosage of DOX was 0.3 mg L^{-1}.

Conclusions

A facile methodology based on a combination of ring-opening polymerizaiton and CuAAC "Click" chemistry was utilized to develop folate (FA)-conjugated and core cross-linked (ACCL-FA) micelles with acid-cleavable acetal groups. The ACCL-FA micelles were prepared by cross-linking of the azide groups on the clickable tetraethylene glycol and the alkynyl groups on the polyphosphoesters (PBYP-*b*-PEEP or PBYP-*b*-PEEP-FA) through CuAAC "Click" reaction. These ACCL micelles exhibited higher values of DLC (11.4%) and DLE (57.2%) than those of the corresponding uncross-linked micelles (UCL), which can be attributed to the improved stability of drug-loaded micelles after cross-linking. The DOX-loaded ACCL micelles exhibited excellent stability in extracellular environments, while they could be fast dissociated in the environment of tumor cells due to the acid-cleavable and enzymatic hydrolysis of polymeric carrier, and then released DOX to the diseased region. We have demonstrated that these FA-conjugated core cross-linked micelles have targeted property and effectively deliver DOX into KB cells. In addition, the enzymatic degradation and cytotoxicity tests reveal that these ACCL-FA micelles based on polyphosphoesters possess good biodegradability and biocompatibility. This new kind of folate-conjugated and core cross-linked biodegradable micelles is highly promising for targeted cancer chemotherapy.

Acknowledgements

The authors gratefully acknowledge financial supports from the National Natural Science Foundation of China (21374066 and 21074078), Suzhou Science and Technology Program for Industrial Application Foundation (SYG201429), the Natural Science Foundation of Jiangsu Province (BK20130286), a Project Funded by the Priority Academic Program Development (PAPD) of Jiangsu Higher Education Institutions, and Soochow-Waterloo University Joint Project for Nanotechnology from Suzhou Industrial Park. Mr. Jian Hu would like to thank the financial support from the Innovative Graduate Research Program of Jiangsu Province (KYLX_1222).

Notes and references

College of Chemistry, Chemical Engineering and Materials Science, Suzhou Key Laboratory of Macromolecular Design and Precision Synthesis, Jiangsu Key Laboratory of Advanced Functional Polymer Design and Application, Soochow University, Suzhou 215123, P. R. China. Tel: +86 512 65882047; E-mail: phni@suda.edu.cn

† Electronic Supplementary Information (ESI) available. See DOI: 10.1039/b000000x/

1 G. S. Kwon and T. Okano, *Adv. Drug Delivery Rev.*, 1996, **21**, 107-116.
2 C. Deng, Y. J. Jiang, R. Cheng, F. H. Meng and Z. Y. Zhong, *Nano Today*, 2012, **7**, 467-480.
3 K. Kataoka, A. Harada and Y. Nagasaki, *Adv. Drug Delivery Rev.*, 2012, **64**, 37-48.
4 A. Rösler, G. W. M. Vandermeulen and H. A. Klok, *Adv. Drug Delivery Rev.*, 2012, **64**, 270-279.
5 S. C. Kim, D. W. Kim, Y. H. Shim, J. S. Bang, H. S. Oh, S. W. Kim and M. H. Seo, *J. Control. Release*, 2001, **72**, 191-202.
6 X. T. Shuai, T. Merdan, A. K. Schaper, F. Xi and T. Kissel, *Bioconjugate Chem.*, 2004, **15**, 441-448.
7 T. Y. Kim, D. W. Kim, J. Y. Chung, S. G. Shin, S. C. Kim, D. S. Heo, N. K. Kim and Y. J. Bang, *Clin. Cancer Res.*, 2004, **10**, 3708-3716.
8 Y. Matsumura, T. Hamaguchi, T. Ura, K. Muro, Y. Yamada, Y. Shimada, K. Shirao, T. Okusaka, H. Ueno and M. Ikeda, *Brit. J. Cancer*, 2004, **91**, 1775-1781.
9 P. Opanasopit, M. Yokoyama, M. Watanabe, K. Kawano, Y. Maitani and T. Okano, *Pharmaceut. Res.*, 2004, **21**, 2001-2008.
10 Y. Kakizawa and K. Kataoka, *Adv. Drug Delivery Rev.*, 2002, **54**, 203-222.
11 H. L. Sun, B. N. Guo, R. Cheng, F. H. Meng, H. Y. Liu and Z. Y. Zhong, *Biomaterials*, 2009, **30**, 6358-6366.
12 T. Hamaguchi, Y. Matsumura, M. Suzuki, K. Shimizu, R. Goda, I. Nakamura, I. Nakatomi, M. Yokoyama, K. Kataoka and T. Kakizoe, *Brit. J. Cancer*, 2005, **92**, 1240-1246.
13 F. Koizumi, M. Kitagawa, T. Negishi, T. Onda, S. Matsumoto, T. Hamaguchi and Y. Matsumura, *Cancer Res.*, 2006, **66**, 10048-10056.
14 H. Uchino, Y. Matsumura, T. Negishi, F. Koizumi, T. Hayashi, T. Honda, N. Nishiyama, K. Kataoka, S. Naito and T. Kakizoe, *Brit. J. Cancer*, 2005, **93**, 678-687.
15 R. Plummer, R. H. Wilson, H. Calvert, A. V. Boddy, M. Griffin, J. Sludden, M. J. Tilby, M. Eatock, D. G. Pearson, C. J. Ottley, Y. Matsumura, K. Kataoka and T. Nishiya, *Brit. J. Cancer*, 2011, **104**,

593-598.
16 http://www.nanocarrier.co.jp/en/research/pipeline/03.html
17 W. C. Zamboni, V. Torchilin, A. K. Patri, J. Hrkach, S. Stern, R. Lee, A. Nel, N. J. Panaro and P. Grodzinski, *Clin. Cancer Res.*, 2012, **18**, 3229-3241.
18 R. K. O'Reilly, C. J. Hawker and K. L. Wooley, *Chem. Soc. Rev.*, 2006, **35**, 1068-1083.
19 Z. H. Zhang, L. C. Yin, C. L. Tu, Z. Y. Song, Y. F. Zhang, Y. X. Xu, R. Tong, Q. Zhou, J. Ren and J. J. Cheng, *ACS Macro Lett.*, 2013, **2**, 40-44.
20 K. B. Thurmond II, T. Kowalewski and K. L. Wooley, *J. Am. Chem. Soc.*, 1996, **118**, 7239-7240.
21 H. R. Huang, E. E. Remsen, T. Kowalewski and K. L. Wooley, *J. Am. Chem. Soc.*, 1999, **21**, 3805-3806.
22 Y. T. Li, B. S. Lokitz, S. P. Armes and C. L. McCormick, *Macromolecules*, 2006, **39**, 2726-2728.
23 X. L. Hu, H. Li, S. Z. Luo, T. Liu, Y. Y. Jiang and S. Y. Liu, *Polym. Chem.*, 2013, **4**, 695-706.
24 A. Guo, G. J. Liu and J. Tao, *Macromolecules*, 1996, **29**, 2487-2493.
25 Y. Kakizawa, A. Harada and K. Kataoka, *J. Am. Chem. Soc.*, 1999, **121**, 11247-11248.
26 Y. N. Chan, T. Wong, F. Byrne, M. Kavallaris and V. Bulmus, *Biomacromolecules*, 2008, **9**, 1826-1836.
27 S. M. Garg, X. B. Xiong, C. H. Lu and A. Lavasanifar, *Macromolecules*, 2011, **44**, 2058-2066.
28 T. C. Lai, H. Cho and G. S. Kwon, *Polym. Chem.*, 2014, **5**, 1650-1661.
29 Y. Zhang, C. S. Xiao, M. Q. Li, J. X. Ding, C. L. He, X. L. Zhuang and X. S. Chen, *Polym. Chem.*, 2014, **5**, 2801-2808.
30 Y. Han, J. J. Li, M. H. Zan, S. Z. Luo, Z. S. Ge and S. Y. Liu, *Polym. Chem.*, 2014, **5**, 3707-3718.
31 V. Bütün, X. S. Wang, M. V. de Paz Bánez, K. L. Robinson, N. C. Billingham, S. P. Armes and Z. Tuzar, *Macromolecules*, 2000, **33**, 1-3.
32 H. F. Xu, F. H. Meng and Z. Y. Zhong, *J. Mater. Chem.*, 2009, **19**, 4183-4190.
33 E. S. Lee, Z. G. Gao and Y. H. Bae, *J. Control. Release*, 2008, **132**, 164-170.
34 S. Ganta, H. Devalapally, A. Shahiwala and M. Amiji, *J. Control. Release*, 2008, **126**, 187-204.
35 Y. L. Li, W. J. Du, G. R. Sun and K. L. Wooley, *Macromolecules*, 2008, **41**, 6605-6607.
36 H. S. Oberoi, F. C. Laquer, L. A. Marky, A. V. Kabanov and T. K. Bronich, *J. Control. Release*, 2011, **153**, 64-72.
37 Y. C. Wang, Y. Y. Yuan, J. Z. Du, X. Z. Yang and J. Wang, *Macromol. Biosci.*, 2009, **9**, 1154-1164.
38 Z. Zhao, J. Wang, H. Q. Mao and K. W. Leong, *Adv. Drug Delivery Rev.*, 2003, **55**, 483-499.
39 H. Y. Shao, M. Z. Zhang, J. L. He and P. H. Ni, *Polymer*, 2012, **53**, 2854-2863.
40 J. Z. Du, X. J. Du, C. Q. Mao and J. Wang, *J. Am. Chem. Soc.*, 2011, **133**, 17560-17563.
41 S. Y. Zhang, A. Li, J. Zou, L. Y. Lin and K. L. Wooley, *ACS Macro Lett.*, 2012, **1**, 328-333.
42 J. Y. Liu, W. Huang, Y. Pang, P. Huang, X. Y. Zhu, Y. F. Zhou and D. Y. Yan, *Angew. Chem., Int. Ed.*, 2011, **50**, 9162-9166.
43 J. Baran and S. Penczek, *Macromolecules*, 1995, **28**, 5167-5176.
44 G. Y. Zhang, M. Z. Zhang, J. L. He and P. H. Ni, *Polym. Chem.*, 2013, **4**, 4515-4525.
45 F. Wang, Y. C. Wang, L. F. Yan and J. Wang, *Polymer*, 2009, **50**, 5048-5054.
46 B. I. Dahiyat, M. Richards and K. W. Leong, *J. Control. Release*, 1995, **33**, 13-21.
47 Y. Luo, R. X. Zhuo and C. L. Fan, Chem. *J. Chin. Uni.*, 1995, **16**, 1633-1636.
48 Y. C. Wang, X. Q. Liu, T. M. Sun, M. H. Xiong and J. Wang, *J. Control. Release*, 2008, **128**, 32-40.
49 Y. F. Zhou, W. Huang, J. Y. Liu, X. Y. Zhu and D. Y. Yan, *Adv. Mater.*, 2010, **22**, 4567-4590.
50 X. Z. Yang, J. Z. Du, S. Dou, C. Q. Mao, H. Y. Long and J. Wang, *ACS Nano*, 2012, **6**, 771-781.
51 M. H. Xiong, Y. Bao, X. Z. Yang, Y. C. Wang, B. L. Sun and J. Wang, *J. Am. Chem. Soc.*, 2012, **134**, 4355-4362.
52 G. L. Li, J. Y. Liu, Y. Pang, R. B. Wang, L. M. Mao, D. Y. Yan, X. Y. Zhu and J. Sun, *Biomacromolecules*, 2011, **12**, 2016-2026.
53 J. L. He, M. Z. Zhang and P. H. Ni, *Soft Matter*, 2012, **8**, 6033-6038.
54 Y. Y. Yuan, J. Z. Du, W. J. Song, F. Wang, X. Z. Yang, M. H. Xiong and J. Wang, *J. Mater. Chem.*, 2012, **22**, 9322-9329.
55 M. H. Xiong, Y. Bao. X. J. Du, Z. B. Tan, Q. Jiang, H. X. Wang, Y. H. Zhu and J. Wang, *ACS Nano*, 2013, **7**, 10636-10645.
56 Y. Xiao, J. L. He, Y. F. Tao, M. Z. Zhang, J. Hu and P. H. Ni, *Acta Polym. Sin.*, 2014, **1**, 122-130.
57 J. Wen, G. J. A. Kim and K. W. Leong, *J. Control. Release*, 2003, **92**, 39-48.
58 H. Zhao, Q. J. Chen, L. Z. Hong, L. Zhao, J. F. Wang and C. Wu, *Macromol. Chem. Phys.*, 2011, **212**, 663-672.
59 H. R. Wang, J. L. He, M. Z. Zhang, Y. F. Tao, F. Li, K. C. Tam and P. H. Ni, *J. Mater. Chem. B*, 2013, **1**, 6596-6607.
60 L. B. Luo, J. Tam, D. Maysinger and A. Eisenberg, *Bioconjugate Chem.*, 2002, **13**, 1259-1265.
61 R. Savić, L. B. Luo, A. Eisenberg and D. Maysinger, *Science*, 2003, **300**, 615-618.
62 Y. Y. Diao, H. Y. Li, Y. H. Fu, M. Han, Y. L. Hu, H. L. Jiang, Y. Tsutsumi, Q. C. Wei, D. W. Chen and J. Q. Gao, *Int. J. Nanomed.*, 2011, **6**, 1955-1962.

Graphical Abstract

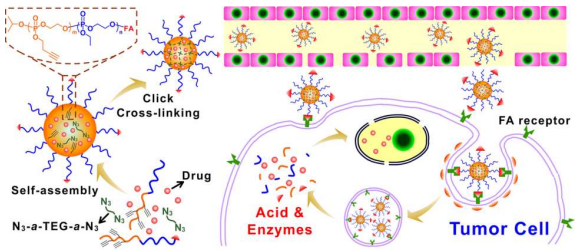

Novel folate-conjugated acid-cleavable core cross-linked polyphosphoester micelles have been prepared and used for pH and enzyme-triggered delivery of doxorubicin.